Eur. Phys. J. B **30**, 239–251 (2002)
DOI: 10.1140/epjb/e2002-00377-4

THE EUROPEAN PHYSICAL JOURNAL B

Infinite chain of N different deltas: A simple model for a quantum wire

J.M. Cerveró[a] and A. Rodríguez

Física Teórica, Facultad de Ciencias, Universidad de Salamanca, 37008 Salamanca, Spain

Received 24 June 2002
Published online 29 November 2002 –

Abstract. We present the exact diagonalization of the Schrödinger operator corresponding to a periodic potential with N deltas of different couplings, for arbitrary N. This basic structure can repeat itself an infinite number of times. Calculations of band structure can be performed with a high degree of accuracy for an infinite chain and of the correspondent eigenlevels in the case of a random chain. The main physical motivation is to modelate quantum wire band structure and the calculation of the associated density of states. These quantities show the fundamental properties we expect for periodic structures although for low energy the band gaps follow unpredictable patterns. In the case of random chains we find Anderson localization; we analize also the role of the eigenstates in the localization patterns and find clear signals of fractality in the conductance. In spite of the simplicity of the model many of the salient features expected in a quantum wire are well reproduced.

PACS. 03.65.-w Quantum mechanics – 71.23.An Theories and models; localized states – 73.21.Hb Quantum wires

Introduction

Quantum wires represent the dreamed idea of make a conductor wire as small as a molecule. The idea that macroscopic devices we have been using for years can actually be built in nature at the nanoscale size goes back to Feynman and is the basis of all work currently carried out in the field of Quantum Electronics. This area of research is not only interesting in itself from the fundamental point of view but has also profound implications in applied physics and material sciences as hundreds of experiments are being carried out nowdays with a high degree of success. The purpose of this paper is to show that some of the ideas underlying the actual development of different types of quantum wires can actually be modelled in quite a simple manner using elementary quantum mechanics. This is specially important from our point of view as it provides a bridge between current fundamental research and basic concepts of quantum mechanics which are usually the subject of graduate standard programs.

The aim to modelate a simple one-dimensional solid in order to study its band structure goes back to Kronig and Penney in the thirties [1] but since then much work has been done along the lines of this first seminal reference. A sample of the variety of models that can be constructed with the same ideas can be found in [2]. As the main interest of almost all of these authors was band theory, the techniques used in all these papers were mainly addressed to semiconductor physics [3]. Much more recently a revival of the same models and techniques [4] has arisen as a consequence of the interest in truly theoretical and experimental one-dimensional physical systems from which quantum wires are just only one example [5]. Right now the research in molecular conductances, one-dimensional metallic rings and other devices of the same sort lends support to the idea of generalizing old methods yielding exact analytic solutions coupled to the use of desk-top computer algebra.

Here firstly we shall solve analytically the band structure of *an infinite periodic chain of delta potentials each one with a different coupling inside the primitive cell* paying mostly attention to the mathematical aspects. After studying the band structure of the chain one can introduce randomness boosted by quantum fluctuations in order to account for localization. Fortunately the model seems rich enough to yield more information such as the generalization of the Saxon-Hutner conjecture [6] and even scaling exhibited as fractal behaviour of the conductance [7]. The paper will be organized as follows. In Section 1 we shall present the analytic solution of **the periodic case** of infinite different delta potentials. The band structure of this one dimensional periodic potential will also be briefly discussed. In Section 2 we turn our attention to the case of **random arrays** of one dimensional delta potentials with different couplings. Here we discuss the density of states using the functional equation method and classify

[a] e-mail: cervero@sonia.usal.es

$$\left(\begin{array}{cc:cc:cc} \mathrm{e}^{\mathrm{i}ka} & \mathrm{e}^{-\mathrm{i}ka} & -1 & -1 & 0 & 0 \\ -\mathrm{i}k\mathrm{e}^{\mathrm{i}ka} & \mathrm{i}k\mathrm{e}^{-\mathrm{i}ka} & (\mathrm{i}k-\frac{2}{a_1}) & -(\mathrm{i}k+\frac{2}{a_1}) & 0 & 0 \\ \hdashline 0 & 0 & \mathrm{e}^{\mathrm{i}ka} & \mathrm{e}^{-\mathrm{i}ka} & -1 & -1 \\ 0 & 0 & -\mathrm{i}k\mathrm{e}^{\mathrm{i}ka} & \mathrm{i}k\mathrm{e}^{-\mathrm{i}ka} & (\mathrm{i}k-\frac{2}{a_2}) & -(\mathrm{i}k+\frac{2}{a_2}) \\ \hdashline -\mathcal{F}_3 & -\mathcal{F}_3 & 0 & 0 & \mathrm{e}^{\mathrm{i}ka} & \mathrm{e}^{-\mathrm{i}ka} \\ (\mathrm{i}k-\frac{2}{a_3})\mathcal{F}_3 & -(\mathrm{i}k+\frac{2}{a_3})\mathcal{F}_3 & 0 & 0 & -\mathrm{i}k\mathrm{e}^{\mathrm{i}ka} & \mathrm{i}k\mathrm{e}^{-\mathrm{i}ka} \end{array}\right). \quad (2)$$

the different types of localization appearing when disorder is present. As we have been able to increase our understanding of localization to the extent of detecting universality effects, we shall entirely devote the Section 3 to the discussion of fractality in the conductance and the different checkings we have managed to perform in order to ascertain ourselves and try to convince the reader that the effect is present even in this extremely simple model. We close with a section of conclusions.

1 Periodic array

Let us consider an electron in a periodic one dimensional chain of atoms modelled by the potential constituted by an array of N delta functions each one with its own coupling e_i^2, $(i = 1, 2, ...N)$. After finishing the N-array, the structure repeats itself an infinite number of times. The number of *species* N, can be arbitrarily large but finite. The case N=1 is an old textbook exercise but may be convenient to be revisited [8] for taking a full profit of our general results. The generalization can thus be followed in a more straightforward manner. The relevant primitive cell (p.c.) for $N = 2$ can be represented for the following set of wavefunctions:

$$p.c. \begin{cases} \Psi_1(x) = A_1\mathrm{e}^{\mathrm{i}kx} + B_1\mathrm{e}^{-\mathrm{i}kx} & 0 \le x < a \\ \Psi_2(x) = A_2\mathrm{e}^{\mathrm{i}k(x-a)} + B_2\mathrm{e}^{-\mathrm{i}k(x-a)} & a \le x < 2a \end{cases}$$
$$\Psi_3(x) = \mathrm{e}^{2\mathrm{i}Qa}\left[A_1\mathrm{e}^{\mathrm{i}k(x-2a)} + B_1\mathrm{e}^{-\mathrm{i}k(x-2a)}\right].$$

The matrix relating the amplitudes of the above wave functions for this $N = 2$ case can be written as:

$$\left(\begin{array}{cc:cc} \mathrm{e}^{\mathrm{i}ka} & \mathrm{e}^{-\mathrm{i}ka} & -1 & -1 \\ -\mathrm{i}k\mathrm{e}^{\mathrm{i}ka} & \mathrm{i}k\mathrm{e}^{-\mathrm{i}ka} & (\mathrm{i}k-\frac{2}{a_1}) & -(\mathrm{i}k+\frac{2}{a_1}) \\ \hdashline -\mathcal{F}_2 & -\mathcal{F}_2 & \mathrm{e}^{\mathrm{i}ka} & \mathrm{e}^{-\mathrm{i}ka} \\ (\mathrm{i}k-\frac{2}{a_2})\mathcal{F}_2 & -(\mathrm{i}k+\frac{2}{a_2})\mathcal{F}_2 & -\mathrm{i}k\mathrm{e}^{\mathrm{i}ka} & \mathrm{i}ke^{-\mathrm{i}ka} \end{array}\right) \quad (1)$$

It is trivial to generalize these two steps to the case of three species (*i.e.* $N = 3$). One can equally write the correspondent matrix in the form:

see equation (2) above

where in all of the above cases, we have used the notation $\mathcal{F}_N = \exp\{\mathrm{i}NQa\}$ and $Q \in \left[-\frac{\pi}{Na}, \frac{\pi}{Na}\right)$, and we shall also be using the *length* of each species, defined as $a_i = \dfrac{\hbar^2}{me_i^2}$. One can now proceed to the generalization of the matrix form for general number N of species just by defining the following 2×2 matrices:

$$\mathbf{E} = \begin{pmatrix} \mathrm{e}^{\mathrm{i}ka} & \mathrm{e}^{-\mathrm{i}ka} \\ -\mathrm{i}k\mathrm{e}^{\mathrm{i}ka} & \mathrm{i}k\mathrm{e}^{-\mathrm{i}ka} \end{pmatrix}; \mathbf{A_j} = \begin{pmatrix} -1 & -1 \\ (\mathrm{i}k-\frac{2}{a_j}) & -(\mathrm{i}k+\frac{2}{a_j}) \end{pmatrix}. \quad (3)$$

The matrices for $N = 2$ and $N = 3$ species given by (1) and (2) can now be put in a more compact form with the help of the $\mathbf{E}$ and $\mathbf{A_j}$ as:

$$\begin{pmatrix} \mathbf{E} & \mathbf{A_1} \\ \mathbf{A_2}\mathcal{F}_2 & \mathbf{E} \end{pmatrix}_{4\times4} \quad ; \quad \begin{pmatrix} \mathbf{E} & \mathbf{A_1} & 0_{2\times2} \\ 0_{2\times2} & \mathbf{E} & \mathbf{A_2} \\ \mathbf{A_3}\mathcal{F}_3 & 0_{2\times2} & \mathbf{E} \end{pmatrix}_{6\times6}. \quad (4)$$

It is now relatively simple to guess that the general form of a matrix for N species must be written as:

$$\begin{pmatrix} \mathbf{E} & \mathbf{A_1} & 0_{2\times2} & \dots & 0_{2\times2} \\ 0_{2\times2} & \mathbf{E} & \mathbf{A_2} & \ddots & \vdots \\ \vdots & \ddots & \ddots & \ddots & 0_{2\times2} \\ \vdots & \ddots & \ddots & \ddots & \mathbf{A_{N-1}} \\ \mathcal{F}\mathbf{A_N} & 0_{2\times2} & \dots & 0_{2\times2} & \mathbf{E} \end{pmatrix}_{2N\times2N}. \quad (5)$$

So far nothing very exciting has happened except that one can write the matrices in a compact, logic and generalizable way. And in fact without further steps the progress would have not been certainly remarkable. The real breakthrough arises when one realizes that one has to deal with the *determinants equated to zero of these matrices* in order to learn something about the *band condition of this one dimensional N-species quantum periodic structure*. Let us

- N even

$$\mathcal{B}(\epsilon; a_1, \ldots, a_N) = 2^{N-1} \sum_P h_i ...(N)... h_k - 2^{N-3} \sum_P h_i ...(N-2)... h_k + 2^{N-5} \sum_P h_i ...(N-4)... h_k - \ldots (-1)^{\frac{N}{2}-1}\, 2 \sum_P h_i ...(2)... h_k + (-1)^{\frac{N}{2}} \tag{8}$$

- N odd

$$\mathcal{B}(\epsilon; a_1, \ldots, a_N) = 2^{N-1} \sum_P h_i ...(N)... h_k - 2^{N-3} \sum_P h_i ...(N-2)... h_k + 2^{N-5} \sum_P h_i ...(N-4)... h_k - \ldots (-1)^{\frac{N-3}{2}}\, 2^2 \sum_P h_i ...(3)... h_k + (-1)^{\frac{N-1}{2}} (h_1 + h_2 + h_3 + \ldots + h_N). \tag{9}$$

---

define the following function ($\epsilon = ka$)[1]:

$$h_i(\epsilon) = \cos(\epsilon) + \left(\frac{a}{a_i}\right) \frac{\sin(\epsilon)}{\epsilon}\,. \tag{6}$$

A quite simple computer algebra calculation shows that the determinant equated to zero of (1), which belongs to the $N = 2$ case, can be written in terms of these functions as

$$\cos(2Qa) = 2\, h_1 h_2 - 1.$$

And the determinant of the $N = 3$ matrix given by (2) can also be calculated to yield:

$$\cos(3Qa) = 4\, h_1 h_2 h_3 - (h_1 + h_2 + h_3).$$

Below, the cases $N = 4, 5, 6$ and 7 are explicitely listed, using the generalized matrix (5) for each case and calculating the determinant equated to zero with the help of the $h(\epsilon)$ functions (6). The result is:

$$\cos(4Qa) = 8\, h_1 h_2 h_3 h_4 - 2\left(h_1 h_2 + h_1 h_4 + h_2 h_3 + h_3 h_4\right) + 1$$

$$\cos(5Qa) = 16\, h_1 h_2 h_3 h_4 h_5 - 4\left(h_1 h_2 h_3 + h_1 h_2 h_5 + h_1 h_4 h_5 + h_2 h_3 h_4 + h_3 h_4 h_5\right) + \left(h_1 + h_2 + h_3 + h_4 + h_5\right)$$

$$\cos(6Qa) = 32\, h_1 h_2 h_3 h_4 h_5 h_6 - 8\left(h_1 h_2 h_3 h_4 + h_1 h_2 h_3 h_6 + h_1 h_2 h_5 h_6 + h_1 h_4 h_5 h_6 + h_2 h_3 h_4 h_5 + h_3 h_4 h_5 h_6\right) + 2\left(h_1 h_2 + h_1 h_4 + h_1 h_6 + h_2 h_3 + h_2 h_5 + h_3 h_4 + h_3 h_6 + h_4 h_5 + h_5 h_6\right) - 1$$

$$\cos(7Qa) = 64\, h_1 h_2 h_3 h_4 h_5 h_6 h_7 - 16\left(h_1 h_2 h_3 h_4 h_5 + h_1 h_2 h_3 h_4 h_7 + h_1 h_2 h_3 h_6 h_7 + h_1 h_2 h_5 h_6 h_7 + h_1 h_4 h_5 h_6 h_7 + h_2 h_3 h_4 h_5 h_6 + h_3 h_4 h_5 h_6 h_7\right) + 4\left(h_1 h_2 h_3 + h_1 h_2 h_5 + h_1 h_2 h_7 + h_1 h_4 h_5 + h_1 h_4 h_7 + h_1 h_6 h_7 + h_2 h_3 h_4 + h_2 h_3 h_6 + h_2 h_5 h_6 + h_3 h_4 h_5 + h_3 h_4 h_7 + h_3 h_6 h_7 + h_4 h_5 h_6 + h_5 h_6 h_7\right) - \left(h_1 + h_2 + h_3 + h_4 + h_5 + h_6 + h_7\right).$$

[1] Notice that for negative energies ϵ takes pure imaginary values that we represent in the figures in the negative part of the spectrum.

We have been able to proof by induction that the general form of the N species case can be given as:

$$\cos(NQa) \;=\; \mathcal{B}(\epsilon; a_1, \ldots, a_N) \tag{7}$$

see equations (8–9) above

All what remains is to define the symbol $\sum_P h_i ...(M)... h_k$ which means the *sum of all possible products of M different h_i's with the following rule for each product: the indices must follow an increasing order and to an odd index must always follow an even index and reciprocally.*

The band structure provided by (8) and (9) is not just **exact** but also extremely useful from the point of view of computer algebra calculations. In fact we have carried out various profiles for the curves provided for these conditions until $N = 30$ or more using just few seconds of a lap-top regular computer. The reason for that lies mainly in the systematic use of the form, products and combinations of the $h(\epsilon)$-function defined by (6). As examples of what has just been said we list in Figure 1 a series of band curves for large number of species and various values of the parameter $\left(\frac{a}{a_i}\right)$, defining the characteristic value of the $h(\epsilon)$-function. One can observe also the unpredictable set of allowed bands which appear at low energies. This pattern increases its unpredictibility with the number of species.

Once the band condition is known, one can write the distribution of electronic states in a very simple form. In one dimension the density of states per unit length of the chain for the n*th* band comes from,

$$g_n(\epsilon) \;=\; \frac{1}{2\pi} \sum_Q \left| \frac{\mathrm{d}\epsilon(Q)}{\mathrm{d}Q} \right|^{-1} \tag{10}$$

where the sum is over all the first Brillouin zone (1BZ) points Q with the same energy ϵ. Due to the parity of $\cos(NQa)$ the number of points with the same value of ϵ in the 1BZ is always 2, and provided that overlapping of neighbouring bands is not possible in this system, we can write the density of states as

$$g(\epsilon) \;=\; \frac{1}{\pi} \left| \frac{\mathrm{d}Q(\epsilon)}{\mathrm{d}\epsilon} \right| \tag{11}$$

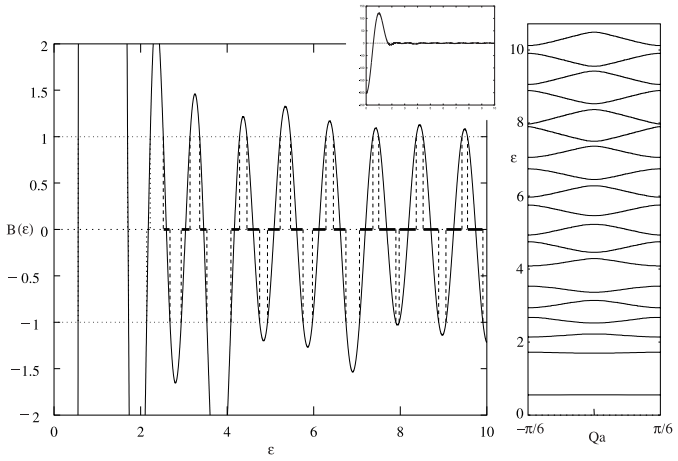

(a) Six species $\left(\frac{a}{a_i}\right)$: 2, 2.5, 1, 1.5, −1, −2.

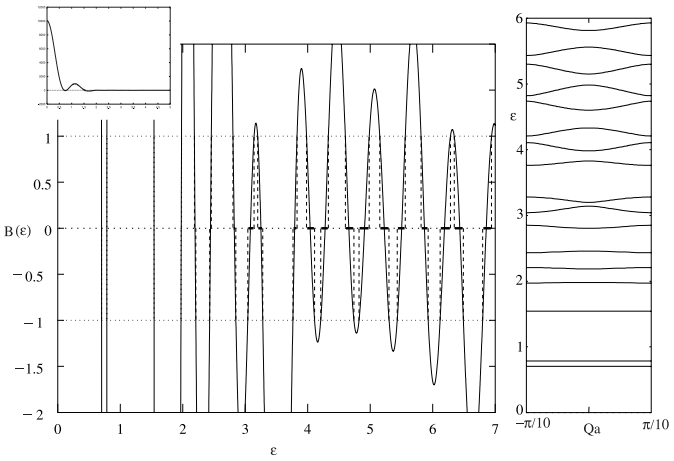

(b) Ten species $\left(\frac{a}{a_i}\right)$: 1, 2, 3, −1, −2, −3,0.5, −0.5, 2, 1.

Fig. 1. Band condition (thick lines mark the allowed energies and the upper small boxes show the whole image of $\mathcal{B}(\epsilon)$) and band structure in 1BZ (vertical diagram) for a periodic chain with different configurations of the primitive cell.

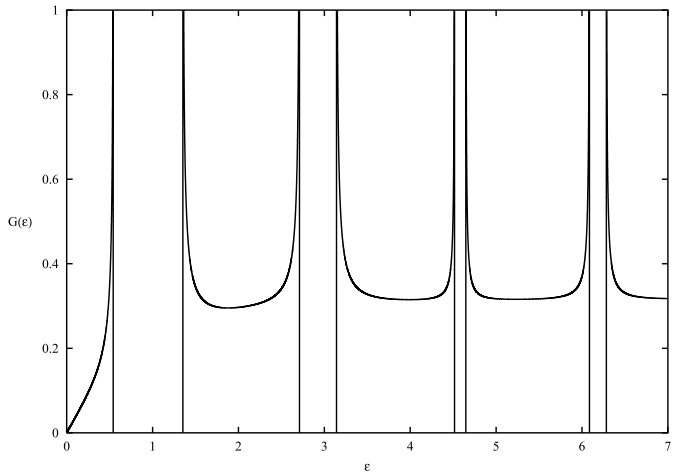

(a) Two species $\left(\frac{a}{a_i}\right)$: −0.3, −0.9.

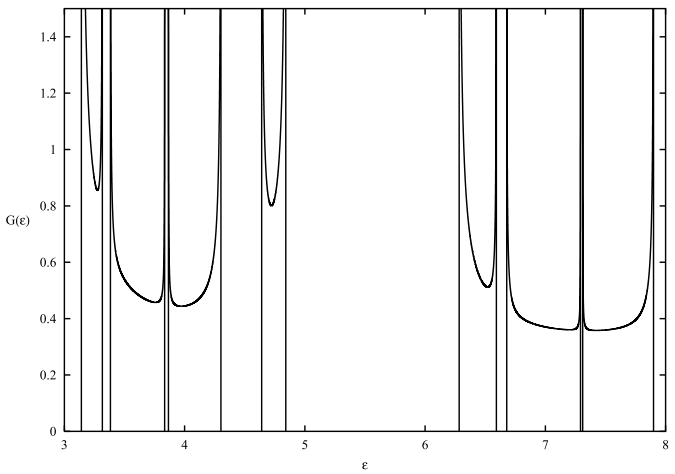

(b) Four species $\left(\frac{a}{a_i}\right)$: −3, −5, −6, −4.

Fig. 2. Density of electronic states for different configurations of the primitive cell.

inside the permitted bands. From (7) a trivial calculation leads to,

$$G(\epsilon) \equiv g(\epsilon)a = \frac{\left[1-\mathcal{B}^2\right]^{-\frac{1}{2}}}{N\pi}\left|\frac{\mathrm{d}\mathcal{B}(\epsilon)}{\mathrm{d}\epsilon}\right| \qquad (12)$$

where $G(\epsilon)$ is the density of electronic states per atom. Figure 2 shows some examples of the characteristic form of the distribution of states for different configurations of the primitive cell.

2 Random chains

The structures one can observe in Nature hardly show a perfect periodicity. Even in the laboratory it is a difficult task to grow a crystal free of impurities, vacancies or dislocations. We shall now treat the presence of substitutional disorder in one dimensional delta-potential chains, that is we consider a chain of equally spaced deltas in which the sequence of different species does not obey a periodic pattern. This model has been mainly studied regarding the vibrational spectrum [2], paying less attention to its electronic density of states [9]. For the purpose of studying quantum wires the relevant behaviour we want to analize lies more in the latter than in the former physical property.

2.1 Energy gaps

The Saxon and Hutner conjecture [6] was proved by Luttinger for the case of binary chains [10]. We have been able to extend it to the general case. A detailed calculation

- N **even**

$$\mathcal{A}(\epsilon; a_1, \ldots, a_N) = 2^N (h_1 \cdot \ldots \cdot h_N) - 2^{N-2} \sum_P{}' h_i ... (N-2) ... h_k + 2^{N-4} \sum_P{}' h_i ... (N-4) ... h_k - \ldots (-1)^{\frac{N}{2}-1} 2^2 \sum_P{}' h_i ... (2) ... h_k + (-1)^{\frac{N}{2}} \tag{16}$$

- N **odd**

$$\mathcal{A}(\epsilon; a_1, \ldots, a_N) = 2^{N-1} (h_1 \cdot \ldots \cdot h_N) - 2^{N-3} \sum_P{}' h_i ... (N-2) ... h_k + 2^{N-5} \sum_P{}' h_i ... (N-4) ... h_k - \ldots (-1)^{\frac{N-3}{2}} 2^2 \sum_P{}' h_i ... (3) ... h_k + (-1)^{\frac{N-1}{2}} (h_1 + h_3 + h_5 + \ldots + h_{N-2} + h_N) \tag{17}$$

---

following the line of Schmidt [11] can be found in Appendix A. The result can be easily summarized as follows: *the forbidden bands that coincide in different one species delta chains with couplings $e_1^2, \ldots, e_N^2$ are also forbidden levels in any infinite chain made up of deltas of the N types.* This conclusion can be applied to both disordered and periodic chains. As can be seen in the calculations the result requires the interatomic distances of the chains involved to be constant and the same for all of them.

2.2 Eigenenergies for finite disorder chains

Let us calculate the allowed energy levels of a finite non-periodic chain of deltas with fixed end-points boundary conditions. The procedure to follow is the same as for the periodic case but imposing the vanishing of the wave function at the end-points of the chain which we locate at one atomic distance to the left of the first delta and to the right of the last one. The connection of the wave function throughout the different sectors leads us to a condition for the permitted energy levels in the form of the determinant of a matrix equated to zero. Again these matrices can be written in a generalizable way, so for N deltas we have

$$\begin{pmatrix} \mathbf{E} & \mathbf{A_1} & 0_{2\times2} & \ldots & \ldots & 0_{2\times2} \\ 0_{2\times2} & \mathbf{E} & \mathbf{A_2} & 0_{2\times2} & \ldots & 0_{2\times2} \\ \vdots & 0_{2\times2} & \mathbf{E} & \mathbf{A_3} & 0_{2\times2} & \ldots \\ \vdots & \vdots & 0_{2\times2} & \ddots & \ddots & \ddots \\ \vdots & \vdots & \vdots & \ddots & \ddots & \ddots \\ 0_{2\times2} & \vdots & \vdots & & \ddots & \mathbf{E} \\ \mathbf{U} & 0_{2\times2} & 0_{2\times2} & \ldots & \ldots & \mathbf{V} \end{pmatrix}_{\substack{2(N+1) \\ \times \\ 2(N+1)}} \tag{13}$$

whith $\mathbf{E}$ and $\mathbf{A_j}$ defined in (3) and

$$\mathbf{U} = \begin{pmatrix} 1 & 1 \\ 0 & 0 \end{pmatrix} \qquad \mathbf{V} = \begin{pmatrix} 0 & 0 \\ \mathrm{e}^{\mathrm{i}ka} & \mathrm{e}^{-\mathrm{i}ka} \end{pmatrix} . \tag{14}$$

We found the condition to be factorizable in terms of the functions $h_j(\epsilon)$ in a similar manner to that of the periodic chain.

The eigenenergies of the system are the roots of:

$$\sin(\epsilon) \mathcal{A}(\epsilon; a_1, \ldots, a_N) = 0 \tag{15}$$

where

see equations (16–17) above

and here the symbol $\sum_P{}' h_i ... (M) ... h_k$ means the *sum of all possible products of M different h_i's with the following rule for each product: the first index has to be odd, the indices must follow an increasing order and to an odd index must always follow an even index and reciprocally.*

From (15) we see that $\epsilon = n\pi\,;\, n \in \mathbb{N}$, are always eigenvalues of any finite length disordered chain whatever the species in it.

2.3 Density of electronic states for an infinite chain

The basic assumption concerning the electronic energies of a random chain is that the distribution of levels converges to a limiting distribution as the number of atoms goes to infinity, which is the same for almost all atomic sequences (except for a fraction that goes to zero as $N \to \infty$) as long as the concentrations of the different species remain fixed. The existence of this property is needed by the thermodynamic limit: all quantities charaterizing macroscopically a random infinite chain with fixed species and concentrations cannot depend on the order of any finite-length piece of it. The method used to obtain the density of states in random chains is essentially due to James and Ginzbarg [12] and Schmidt [11], who derived a functional equation which supplies the limiting distribution for the positive part of the spectrum. We have reconstructed and extended the method to provide the density of states for

all energies (Appendix B). The functional equation is,

$$\mathbf{W}(\varphi) = \sum_{i=1}^{m} p_i \left\{ \mathbf{W}\left(\mathcal{T}_i^{-1}(\varphi)\right) - \mathbf{W}\left(\mathcal{T}_i^{-1}(0)\right) \right\} \tag{18a}$$

$$\mathbf{W}(\varphi + r\pi) = \mathbf{W}(\varphi) + r \tag{18b}$$

$$\mathbf{W}(\pi) = 1 \tag{18c}$$

$$\mathbf{W}(\varphi) \text{ is monotonically increasing in } \varphi \tag{18d}$$

where $\varphi \in (0, \pi]$ and m is the number of species composing the chain , p_i the ith species concentration and $\mathcal{T}_i^{-1}(\varphi)$ are the functions,

$$\mathcal{T}_i^{-1}(\varphi) = \arctan\left(2h_i(\epsilon) - \frac{1}{\tan(\varphi)}\right) \tag{19}$$

with $h_i(\epsilon)$ defined in (6). Solving (18) for different values of the energy, the density of electronic states per atom can be obtained from,

$$G(\epsilon) = \frac{\left|\mathcal{K}\left(\epsilon + \frac{\Delta\epsilon}{2}\right) - \mathcal{K}\left(\epsilon - \frac{\Delta\epsilon}{2}\right)\right|}{\Delta\epsilon} \tag{20}$$

where $\mathcal{K} = -\sum_{i=1}^{m} p_i \left[\mathbf{W}\left(\mathcal{T}_i^{-1}(0)\right)\right]$.

We solve this equation numerically. The range of φ is discretized in p equally spaced points and $\mathbf{W}$ is represented by its values at those points which using a selfconsistent algorithm we have been able to calculate up to an error of 10^{-15}. Some examples of distributions for random chains are shown in Figure 3.

The most interesting feature of the different spectra is the localized peak structure that appears for certain energy intervals. Those irregularities had been reported several years ago [9,13] and now the extremely accurate numerical algorithms dramatically confirm. Although the general interpretation of the behaviour of the distributions for these systems is non trivial one can say as a general rule (and following the suggestion of Agacy and Borland [9]) that the peaked regions are remarkable in ranges of the spectrum which are forbidden for some of the species involved but not for all of them since in this latter case the range is also not allowed for the random system. A clear view of this explanation can be obtained by looking at a random chain of two species A and B. In a region forbidden for the A-type chain the allowed energies appearing in the spectrum are due to atomic clusters involving B atoms. As a result the A atoms surrounding these groups isolate those energies causing the density of states to decrease when we move in a tiny region around each of the levels and therefore giving rise to a fluctuating distribution. Thus one could reproduce the energies where the density of states would be more prominent, from the eigenvalues of certain atomic clusters in which the B species have a substantial contribution as shown in Figure 4. In the (a) example it is clear how the eigenstates clusterize around the more peaked regions of the distribution. However one needs to consider a huge number of clusters in order to reproduce all the maxima due to the equal concentrations of the species. Decreasing the B concentration we see in (b) how the sharp points can be quite easily predicted.

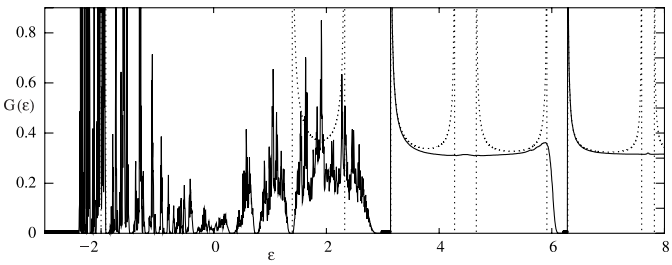

(a) 2 species. $\left(\frac{a}{a_i}\right)\{p_i\} : -2\{0.5\}, -0.25\{0.5\}$. The dotted line is the density of states for the ordered diatomic chain.

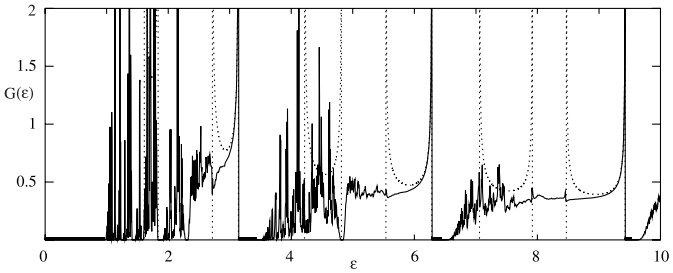

(b) 2 species. $\left(\frac{a}{a_i}\right)\{p_i\} : 6\{0.5\}, 0.5\{0.5\}$. The dotted line is the density of states for the ordered diatomic chain.

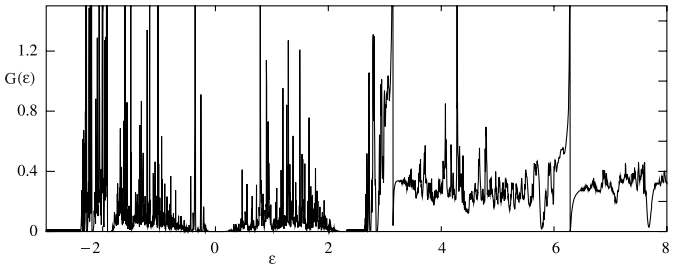

(c) 3 species. $\left(\frac{a}{a_i}\right)\{p_i\} : 10\{0.3\}, -1\{0.3\}, \ -2\{0.4\}$.

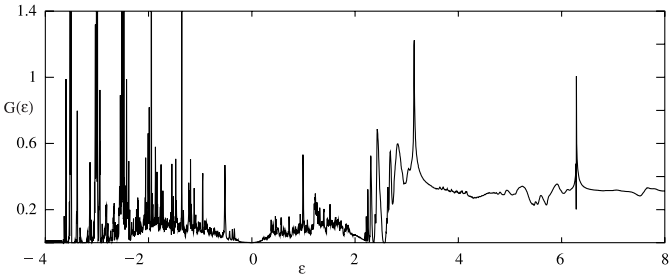

(d) 8 species. $\left(\frac{a}{a_i}\right)\{p_i\} : -0.5\{0.1\}, \ -1\{0.1\}, \ -1.5\{0.1\}, \ -2\{0.1\}, \ -2.5\{0.1\}, \ -3\{0.1\}, \ -3.5\{0.1\}, \ 4\{0.3\}$.

Fig. 3. Distributions of electronic states for different configurations of the random chain. The thick line over the abscisa axis marks the common forbidden bands for the species composing the array. 5001 points have been taken for φ and $\Delta\epsilon = 4\times10^{-3}$.

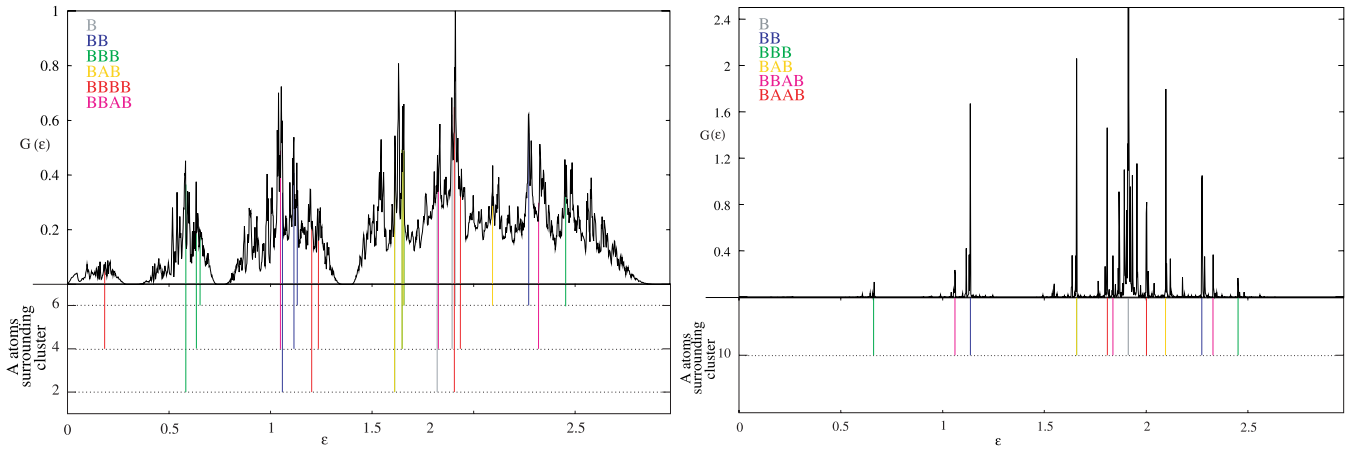

(a) $p_A = p_B = 0.5$ (b) $p_A = 0.9$, $p_B = 0.1$

Fig. 4. Density of states for a 2 species random chain with $\left(\frac{a}{a_A}\right) = -2$ and $\left(\frac{a}{a_B}\right) = -0.25$ in a range forbidden for the A-type chain. The color vertical lines indicate the position of the eigenstates of different atomic B-groups surrounded by a certain number of A atoms. 5001 points have been taken for φ and $\Delta\epsilon = 2 \times 10^{-3}$.

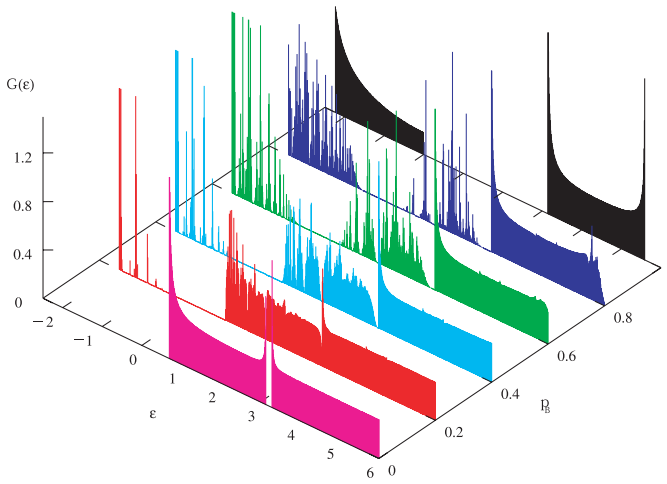

Fig. 5. Distribution of states for 2 species random chains with $\left(\frac{a}{a_A}\right) = 0.25$ and $\left(\frac{a}{a_B}\right) = -2$ in different concentrations. 3001 points have been taken for φ and $\Delta\epsilon = 8 \times 10^{-3}$.

Another feature that can be seen in the different representations in Figure 3, is how the distribution approaches a smoother curve that resembles the one corresponding to a periodic chain as the energy grows: the greater the electron's energy the less it feels the presence of disorder.

In Figure 5, the evolution of the density of states can be observed for a pure one species chain as we dope substitutionally with atoms of a different kind.

2.4 The degree of localization of the electronic states

Since Anderson [14] the disorder in the structures has been accepted as the main effect responsible of the spatial localization of the eigenstates of the systems. Just few years ago it was shown how if the disorder is correlated the localization can be suppressed for certain energies [15,16]. In 1999 the first experimental evidence that correlations inhibit localization of states in disordered low-dimensional systems was reported [17].

Let us check the degree of localization for the electronic states in random chains with positive energy. What we specifically calculate is the average logarithmic decay per atom of the square of the envelope of the real wave function which seems an adequate quantity for such a characterization [18].

In the jth sector we write:

$$\Psi_j(x) = A_j \cos\left(kx - k(j-1)a + \phi_j\right) \tag{21}$$

and we look for:

$$\lim_{N\to\infty} \frac{1}{N} \sum_{j=1}^{N} \log\left(\frac{A_{j+1}^2}{A_j^2}\right). \tag{22}$$

The connection equations of the wave function at the borders of the different sectors imply:

$$\frac{A_{j+1}^2}{A_j^2} = 1 + \left(\frac{2}{ka_j}\right)^2 \cos^2(ka + \phi_j) - \left(\frac{2}{ka_j}\right) \sin(2ka + 2\phi_j). \tag{23}$$

Again, we will be using the functional equation to carry out the calculation so using the phase φ_j as in Appendix B, it is just a matter of algebra to obtain:

$$\begin{aligned} F(\varphi_j, a_j) \equiv \frac{A_{j+1}^2}{A_j^2} &= 1 + \left(\frac{2}{ka_j}\right)^2 \frac{\sin^2(ka)}{1 - 2\cos(ka)\tan(\varphi_j) + \tan^2(\varphi_j)} \\ &+ \left(\frac{2}{ka_j}\right) \frac{2\sin(ka)\big(\cos(ka) - \tan(\varphi_j)\big)}{1 - 2\cos(ka)\tan(\varphi_j) + \tan^2(\varphi_j)} \end{aligned} \tag{24}$$

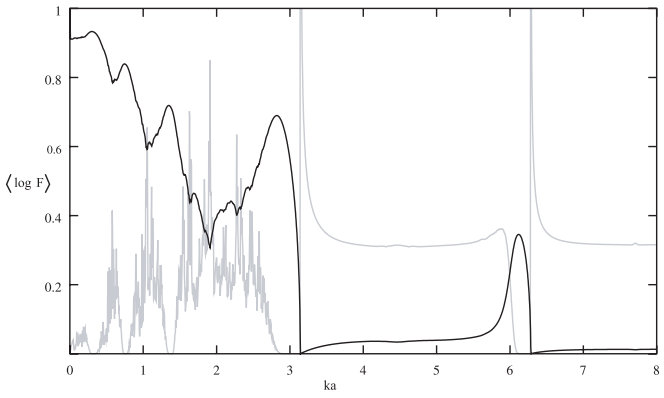

(a) 2 species $\left(\frac{a}{a_1}\right) = -2$ and $\left(\frac{a}{a_2}\right) = -0.25$ with equal concentrations.

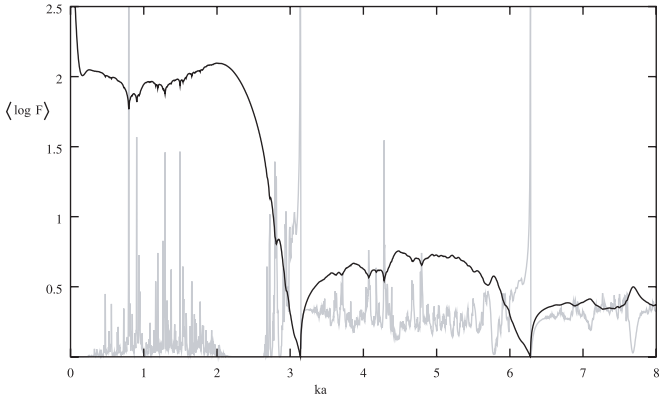

(b) 3 species $\left(\frac{a}{a_1}\right) = 10$, $\left(\frac{a}{a_2}\right) = -1$ and $\left(\frac{a}{a_3}\right) = -2$ with $p_1 = p_2 = 0.3$ and $p_3 = 0.4$.

Fig. 6. Degree of localization for the electronic states (black line) and density of states (grey line) for a random chain. 5001 points have been taken for φ to solve the functional equation and $\Delta(ka) = 4 \times 10^{-3}$.

and the same arguments appearing in the appendix lead us to write (22) as

$$\langle \log F \rangle = \sum_{i=1}^{m} p_i \int_0^{\pi} \frac{\mathrm{d}\mathbf{W}(\varphi)}{\mathrm{d}\varphi} \log F(\varphi, a_i) \mathrm{d}\varphi. \qquad (25)$$

Integrating by parts and using the equations for $\mathbf{W}(\varphi)$, we finally obtain:

$$\langle \log F \rangle = \sum_{i=1}^{m} p_i \log F(\pi, a_i) - \sum_{i=1}^{m} p_i \int_0^{\pi} \mathbf{W}(\varphi) \frac{1}{F(\varphi, a_i)} \frac{\mathrm{d}F(\varphi, a_i)}{\mathrm{d}\varphi} \mathrm{d}\varphi. \qquad (26)$$

In the Figure 6 some examples of the degree of localization as a function of the energy are shown. As can be seen the degree of localization has a tendency to decrease in the peaks of the spectrum and increase in the troughs, and for $ka = n\pi\,;\, n \in \mathbb{N}$ the states are always extended for any chain. This last result had been already obtained using the transfer matrix technique [19] for finite chains. So the system with completely uncorrelated disorder can support extended states. In fact an infinite number of isolated resonances is present although mobility edge for the electrons does not exist and therefore one cannot speak of an Anderson transition in a strict sense for this particularly simple model.

3 Fractality

Let us observe the peaked regions of the distributions. At first sight the irregularities make the density of states appear hardly differentiable within those intervals. Would this pattern still hold as we look deeper into the distribution? Is the distribution non differentiable? In order to answer these questions one has to improve the numerical calculation to be able to see the real density of states in smaller energy ranges. In Figure 7 the spectrum of a certain random chain is shown for shorter and shorter energy intervals. As can be seen as the energy domain is made smaller and thus increasing the accuracy of the numerical algorithm the distribution reveals a finer structure: new sharp points appear and the density does not evolve smoothly. We have been extremely careful with the numerical algorithms and we are pretty sure that the observed irregularities are not due to numerical errors. For the representations in Figure 7 we have proceeded doubling the number of points taken for φ in order to represent the functional equation and checking the convergence of the density of states at each step until the desired accuracy (in all cases the average variation of $G(\epsilon)$ in the last step relative to its domain was less than 0.75%). The final parameters were:

	points for φ	$\Delta\epsilon$
Fig. 7a	5 001	7.5×10^{-4}
Fig. 7b	35 001	2.5×10^{-5}
Fig. 7c	150 001	2.5×10^{-6}

As a final check we repeated the procedure for the same random chain, with the same parameters but in an apparently smooth region of the density of states obtaining the results shown in Figure 8. From this we can see that the irregularities in certain intervals of the spectrum are not due to errors of the numerical computation.

The numerical calculation of the density of states suggests the possibility for the distributions to show a quasi-fractal behaviour in some energy ranges: non differentiability for any point inside these regions and irregular aspect whatever the scale. The differentiability of the distribution is a consequence of a regular (almost homogeneous) distribution of the states inside a small energy interval. A clear view of the differences between the way in which states appear inside an irregular region and a smooth region of the density can be obtained representing the energy spaces for adjacent levels. In Figure 9 these spacing distributions are shown for the first 100 levels that appear inside an irregular zone and a smooth one for a finite length array.

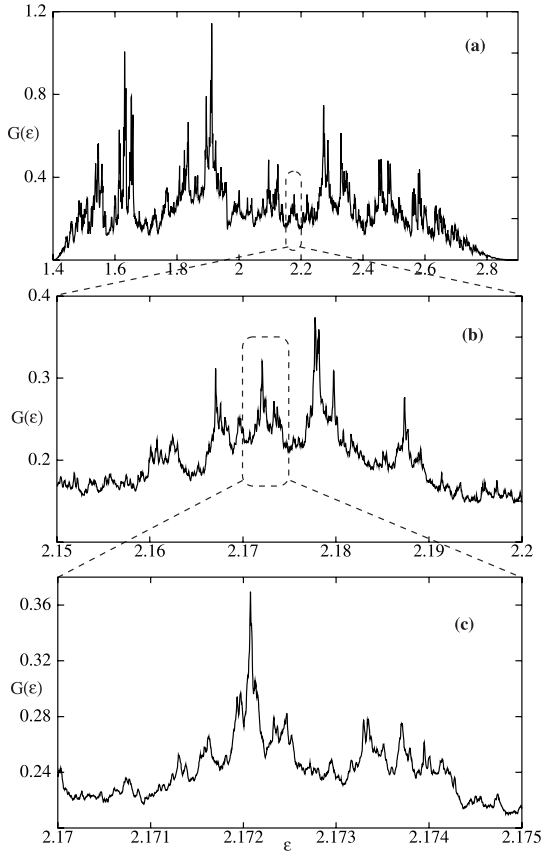

Fig. 7. Density of electronic states in different energy ranges for a two species random chain $\left(\frac{a}{a_1}\right) = -2$ and $\left(\frac{a}{a_2}\right) = -0.25$ with equal concentrations (fractal region).

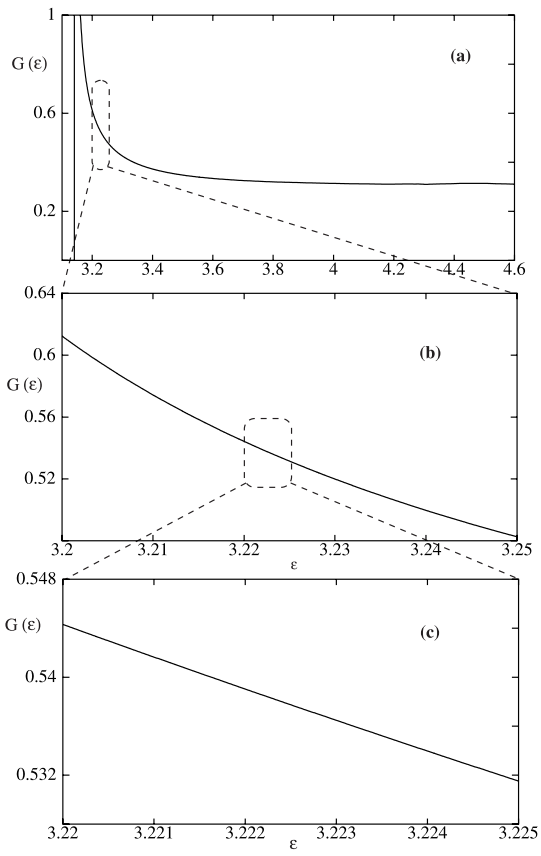

Fig. 8. Density of electronic states in different energy ranges for a two species random chain $\left(\frac{a}{a_1}\right) = -2$ and $\left(\frac{a}{a_2}\right) = -0.25$ with equal concentrations (smooth region).

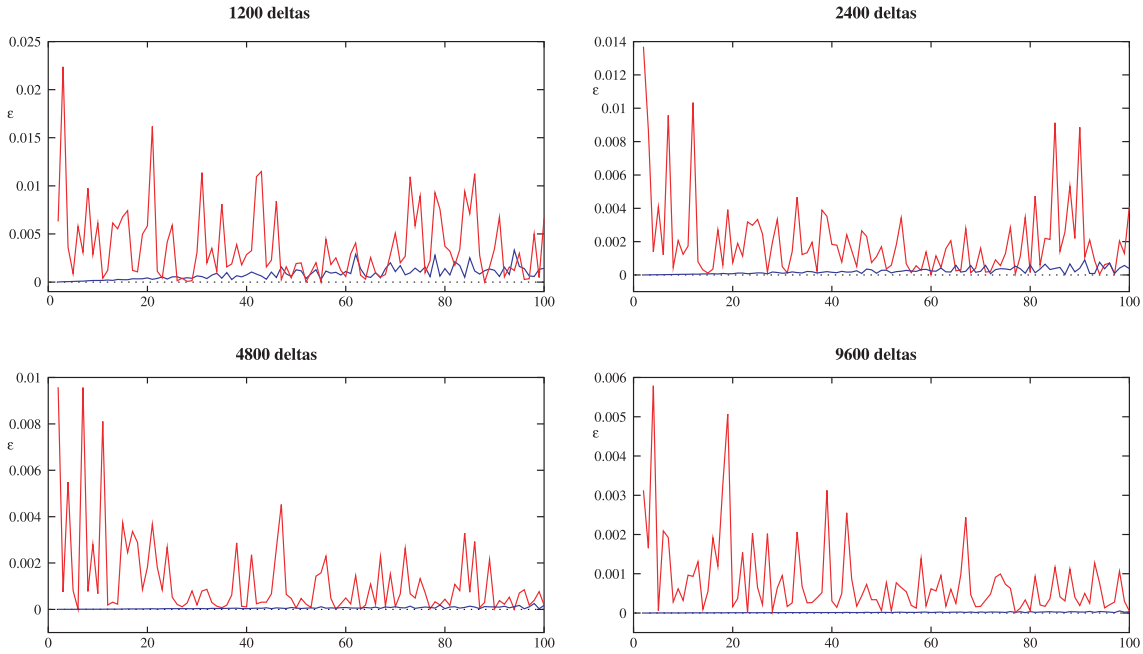

Fig. 9. Energy spacings for the first 100 eigenvalues appearing inside an irregular zone ($\epsilon > 1.4$, red) and inside a regular one ($\epsilon > \pi$, blue). The point n on the abscisa axis represents the energy distance between the $(n-1)$ and n level. All the sequences are composed of the species $\left(\frac{a}{a_1}\right) = -2$ and $\left(\frac{a}{a_2}\right) = -0.25$ with equal concentrations. For a fixed length all the states calculated correspond to the same random sequence. The states have been calculated by finding the transmission of the wave function through the chain with fixed end-points boundary conditions.

Increasing the length of the random chain we see how the spacing distribution for the levels in the smooth region becomes more and more homogeneous as the first 100 levels are included in a smaller energy interval while the spacings for the levels in the irregular zone do not show a defined tendency nor a homogeneous distribution. In fact these last spacing distributions exhibit the same aspect whatever the scale would be. The fractality of the density of states does not depend on any particular parameter of the random chain; its presence is a consequence of the disorder and the dimensionality of the system and it is in this sense a universal effect. This fractal behaviour might be related to the fractal conductance fluctuations observed in gold nanowires [7] in the mesoscopic regime suggesting a connection between disorder and coherent transport.

4 Concluding remarks

To summarize we would like to point out the main results we have obtained in this paper. First, we emphasize that the band structure provided by (7–9) is not just **exact** but also extremely useful from the point of view of computer algebra calculations. In fact we have carried out various profiles for the curves provided for these conditions until N=30 or more using just few seconds of a lap-top regular computer. The reason for that lies mainly in the systematic use of the form, products and combinations of the $h(\epsilon)$-function defined by (6). The Luttinger theorem has been generalized to an arbitrary number of different delta potentials and the Saxon-Hutner Conjecture has also been definitively established. Similar expressions have been obtained for the case of a disordered finite chain and the extended functional equation method has been used to look specifically to the density of electronic states for a random infinite array. By obtaining the degree of localization of the electronic states in the random chains, we have a more complete picture of the role the levels play in the transport processes and the existence of extended states under uncorrelated disorder has been confirmed. The results are not only in agreement with what was expected in more sophisticated models but also go beyond them and we can account for universal properties of the transport effects by detecting fractality in the conductance. This work is far from being finished as we want to ascertain ourselves whether this effect can be measurable in terms of the fractal dimension and critical exponents. At the moment, however, we can already offer a large bundle of properties that arise from a model whose simplicity is not only a shortcoming but rather an advantage to study complex properties in a benchproof easily manageable.

Appendix A: Gaps theorem

Let us consider a finite chain of N delta potentials of different species with fixed end-points boundary conditions (Fig. 10). Inside the jth sector we write the wave function of the electron

$$\Psi_j(x) = A_j \mathrm{e}^{\mathrm{i}kx_j} + B_j \mathrm{e}^{-\mathrm{i}kx_j}, \tag{A.1}$$

where $x_j = x - (j-1)a$.

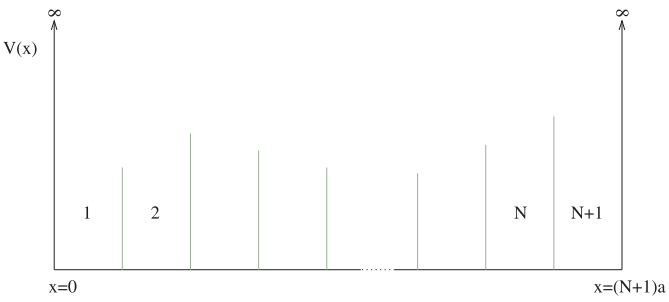

Fig. 10. Deltas chain.

Imposing the conditions at the border $x = ja$ one can obtain the relationship between the amplitudes of adjacent sectors:

$$\begin{pmatrix} A_{j+1} \\ B_{j+1} \end{pmatrix} = \underbrace{\begin{pmatrix} (1 - \frac{\mathrm{i}}{ka_j})\mathrm{e}^{\mathrm{i}ka} & \frac{-\mathrm{i}}{ka_j}\mathrm{e}^{-\mathrm{i}ka} \\ \frac{\mathrm{i}}{ka_j}\mathrm{e}^{\mathrm{i}ka} & (1 + \frac{\mathrm{i}}{ka_j})\mathrm{e}^{-\mathrm{i}ka} \end{pmatrix}}_{M} \begin{pmatrix} A_j \\ B_j \end{pmatrix} \tag{A.2}$$

and M is the transmission matrix of the sectors. The boundary conditions are:

$$A_1 + B_1 = 0 \tag{A.3a}$$

$$A_{N+1}\mathrm{e}^{\mathrm{i}ka} + B_{N+1}\mathrm{e}^{-\mathrm{i}ka} = 0. \tag{A.3b}$$

Let us define inside each sector $\tau_j = -\mathrm{i}\mathrm{e}^{ika}\dfrac{A_j}{B_j}$. Equations (A.3) become:

$$\tau_1 = \mathrm{i}\mathrm{e}^{\mathrm{i}ka} \tag{A.4a}$$

$$\tau_{N+1} = \mathrm{i}\mathrm{e}^{-\mathrm{i}ka}, \tag{A.4b}$$

and from (A.2) the transmission for τ_j is

$$\tau_{j+1} = \frac{c_j\tau_j + 1}{\tau_j + c_j^*} \tag{A.5}$$

where $c_j = (\mathrm{i} - ka_j)\mathrm{e}^{\mathrm{i}ka}$. Let us use $z_j = \dfrac{\mathrm{e}^{\mathrm{i}ka} + \mathrm{i}\tau_j}{1 + \mathrm{i}\tau_j\mathrm{e}^{\mathrm{i}ka}}$. The boundary conditions now read:

$$z_1 = 0 \tag{A.6a}$$

$$z_{N+1} = \infty. \tag{A.6b}$$

A straightforward calculation using (A.5) lead us to:

$$z_{j+1} = \frac{1}{2h_j(ka) - z_j}\,. \tag{A.7}$$

with $h_j(ka) = \cos(ka) + \left(\frac{a}{a_j}\right)\dfrac{\sin(ka)}{ka}$. Now let us consider the values of ka satisfying $|h_j(ka)| > 1$ for every a_j in the chain (*i.e.* the common forbidden bands for all the one species chains). As $|z_1| < 1$ it is easy to proof by

induction using (A.7) that $|z_j| < 1 \Rightarrow |z_{j+1}| < 1$. So we have $|z_{N+1}| < 1$ for arbitrary N and the final boundary condition cannot be satisfied whatever the length of the chain. Therefore those ka values are not allowed in the mixed chain. Notice that the order in which the different species appear is irrelevant. The same conclusion holds for both periodic and disordered chains.

The result is also valid for complex values of k (*i.e.* negative energies).

Appendix B: Functional equation

The limiting distribution of electronic states for a random chain composed of m different species each one with concentration p_i, will be given by the average of the spectra for all sequences which have the given concentrations in the limit as the number of atoms goes to infinity.

Let us consider the same chain as in Appendix A and the quantities z_j. Since $z_1 = 0$ and the transmission (A.7) is real, every z_j will also be real and we can define a phase in each sector φ_j so that $\tan(\varphi_j) = z_j$, which yields the result:

$$\varphi_{j+1} \equiv \mathcal{T}_j(\varphi_j) \;=\; \arctan\left(\frac{1}{2h_j(\epsilon) - \tan(\varphi_j)}\right). \qquad \text{(B.1)}$$

We need the transmission of the phase to be an increasing continuous function. Thus we define:

$$\mathcal{T}_j(\varphi_j) = \begin{cases} \arctan\left(\frac{1}{2h_j(\epsilon)-\tan(\varphi_j)}\right) \\ \qquad\qquad \text{if } \varphi_j \in \left(-\frac{\pi}{2}, \arctan\big(2h_j(\epsilon)\big)\right] \\ \arctan\left(\frac{1}{2h_j(\epsilon)-\tan(\varphi_j)}\right) + \pi \\ \qquad\qquad \text{if } \varphi_j \in \left(\arctan\big(2h_j(\epsilon)\big), \frac{\pi}{2}\right] \end{cases} \qquad \text{(B.2)}$$

$$\mathcal{T}_j(\varphi_j + n\pi) = \mathcal{T}_j(\varphi_j) + n\pi \qquad \varphi_j \in \left(-\frac{\pi}{2}, \frac{\pi}{2}\right]. \qquad \text{(B.3)}$$

This can be easily written by using the inverse function as:

$$\mathcal{T}_j^{-1}(\varphi_j) = \arctan\left(2h_j(\epsilon) - \frac{1}{\tan(\varphi_j)}\right) \qquad \text{(B.4)}$$

$$\mathcal{T}_j^{-1}(\varphi_j + n\pi) = \mathcal{T}_j^{-1}(\varphi_j) + n\pi \qquad \varphi_j \in (0, \pi]. \qquad \text{(B.5)}$$

The boundary conditions are:

$$\varphi_1 = 0 \qquad \text{(B.6)}$$

$$\varphi_{N+1} = \frac{\pi}{2} + n\pi \qquad n \in \mathbb{Z}. \qquad \text{(B.7)}$$

Once the transmission of the phases can be written in a uniquely way, $\varphi_{N+1}(\epsilon)$ is a continuous function of ϵ. Let us assume the latter to be an increasing function. Then if $\epsilon_1 < \epsilon_2$ the quantity $\dfrac{\varphi_{N+1}(\epsilon_2) - \varphi_{N+1}(\epsilon_1)}{\pi}$ is the number of times the final boundary condition has been satisfied from ϵ_1 to ϵ_2 with an error smaller than 1 and therefore it also represents the number of eigenstates in the interval $\epsilon_1 < \epsilon < \epsilon_2$. So it is clear that we can write the density

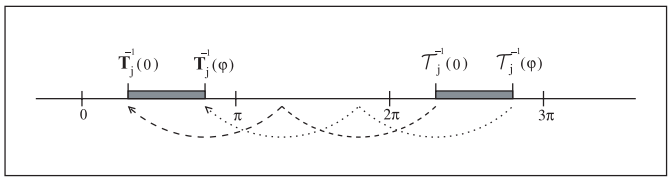

Fig. 11. Example $t = s = 2$.

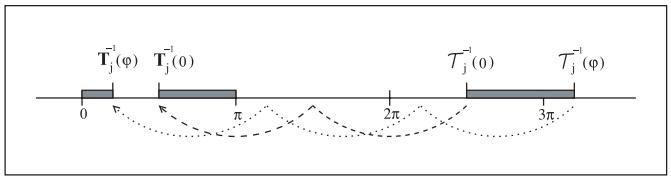

Fig. 12. Example $s = 2$ and $t = 3$.

of states per atom of the chain whatever the behaviour of the function $\varphi_{N+1}(\epsilon)$ would be as:

$$G(\epsilon) = \frac{1}{\pi} \frac{\left| \frac{\varphi_{N+1}(\epsilon+d\epsilon)}{N} - \frac{\varphi_{N+1}(\epsilon)}{N} \right|}{d\epsilon}. \qquad \text{(B.8)}$$

As (B.6) holds for all ϵ, we can write $\frac{\varphi_{N+1}(\epsilon)}{N}$:

$$\frac{\varphi_{N+1}}{N} = \frac{1}{N}\sum_{j=1}^{N}\big[\varphi_{j+1} - \varphi_j\big] = \sum_{j=1}^{N}\frac{\mathcal{T}_j(\varphi_j) - \varphi_j}{N} \qquad \text{(B.9)}$$

for each value of ϵ. Thus $\frac{\varphi_{N+1}(\epsilon)}{N}$ is the average over all atoms of the advanced phase which we denote $\langle \Delta\varphi \rangle(\epsilon)$. As $\mathcal{T}_j(\varphi_j) - \varphi_j$ is a periodic function with period π the average $\langle \Delta\varphi \rangle$ can be calculated using the distribution functions of the phases $\varphi_j(\mod \pi)$.

$$\langle \Delta\varphi \rangle = \frac{1}{N}\sum_{j=1}^{N}\int_0^{\pi} \frac{\mathrm{d}W_j(\varphi)}{\mathrm{d}\varphi}\left\{\mathcal{T}_j(\varphi) - \varphi\right\}\mathrm{d}\varphi \qquad \text{(B.10)}$$

where $W_j(\varphi)$ with $\varphi \in (0, \pi]$ is the probability that $\varphi_j(\mod \pi)$ lies in the interval $(0, \varphi]$. Also we impose:

$$W_j(\varphi + r\pi) = W_j(\varphi) + r \qquad \varphi \in (0, \pi]. \qquad \text{(B.11)}$$

The probability distribution for φ_j depends on the distribution for φ_{j-1}: $\varphi_j(\mod \pi)$ lies in $(0, \varphi]$ if and only if $\varphi_{j-1}(\mod \pi)$ lies in $\left(\mathcal{T}_j^{-1}(0), \mathcal{T}_j^{-1}(\varphi)\right](\mod \pi)$. There exist integers s and t such that

$$\mathcal{T}_j^{-1}(0)(\mod \pi) \equiv \mathbf{T}_j^{-1}(0) = \mathcal{T}_j^{-1}(0) - s\pi \qquad \text{(B.12)}$$

$$\mathcal{T}_j^{-1}(\varphi)(\mod \pi) \equiv \mathbf{T}_j^{-1}(\varphi) = \mathcal{T}_j^{-1}(\varphi) - t\pi \qquad \text{(B.13)}$$

and $0 < \mathcal{T}_j^{-1}(\varphi) - \mathcal{T}_j^{-1}(0) \leq \pi$ from (B.4) thus t must be equal to s or $s+1$.

1. $t = s$
   In this case (Fig. 11):
   $W_j(\varphi) = W_{j-1}\left(\mathbf{T}_j^{-1}(\varphi)\right) - W_{j-1}\left(\mathbf{T}_j^{-1}(0)\right)$.
2. $t = s + 1$
   In this case (Fig. 12):
   $W_j(\varphi) = 1 - W_{j-1}\left(\mathbf{T}_j^{-1}(0)\right) + W_{j-1}\left(\mathbf{T}_j^{-1}(\varphi)\right)$.

Using (B.11) we can unify both cases as $W_j(\varphi) = W_{j-1}\left(\mathcal{T}_j^{-1}(\varphi)\right) - W_{j-1}\left(\mathcal{T}_j^{-1}(0)\right)$. Thus the distribution functions are the solutions of the equations

$$W_j(\varphi) = W_{j-1}\left(\mathcal{T}_j^{-1}(\varphi)\right) - W_{j-1}\left(\mathcal{T}_j^{-1}(0)\right) \quad \text{(B.14a)}$$
$$W_j(\varphi + r\pi) = W_j(\varphi) + r \quad \text{(B.14b)}$$
$$W_j(\pi) = 1 \quad \text{(B.14c)}$$
$$W_j(\varphi) \text{ is an increasing function of } \varphi \quad \text{(B.14d)}$$

with $\varphi \in (0, \pi]$.

The random chain is composed of m different species with lengths $a_1, \ldots, a_m$ in concentrations $p_1, \ldots, p_m$ ($\sum_{i=0}^{m} p_i = 1$). We have now to take into account all possible sequences which have the given concentrations. Thus we only know the probability of finding certain species in the position $x = ja$ and therefore we must take the average. The equation (B.10) becomes:

$$\langle \Delta\varphi \rangle = \frac{1}{N} \sum_{j=1}^{N} \int_0^{\pi} \frac{\mathrm{d}W_j(\varphi)}{\mathrm{d}\varphi} \sum_{i=1}^{m} p_i \left\{\mathcal{T}_i(\varphi) - \varphi\right\} \mathrm{d}\varphi\,, \quad \text{(B.15)}$$

and the equations for the distribution functions become:

$$W_j(\varphi) = \sum_{i=1}^{m} p_i \left\{W_{j-1}\left(\mathcal{T}_i^{-1}(\varphi)\right) - W_{j-1}\left(\mathcal{T}_i^{-1}(0)\right)\right\} \quad \text{(B.16a)}$$
$$W_j(\varphi + r\pi) = W_j(\varphi) + r \quad \text{(B.16b)}$$
$$W_j(\pi) = 1 \quad \text{(B.16c)}$$
$$W_j(\varphi) \text{ is an increasing function of } \varphi \quad \text{(B.16d)}$$

with $\varphi \in (0, \pi]$. Notice that now $W_j(\varphi)$ is the probability that $\varphi_j(\mod \pi)$ lies in the interval $(0, \varphi]$ in some of the possible sequences. Let us write (B.15) as

$$\langle \Delta\varphi \rangle = \sum_{i=1}^{m} p_i \int_0^{\pi} \frac{\mathrm{d}W^N(\varphi)}{\mathrm{d}\varphi} \left\{\mathcal{T}_i(\varphi) - \varphi\right\} \mathrm{d}\varphi \quad \text{(B.17)}$$

where $W^N(\varphi) = \frac{1}{N} \sum_{j=1}^{N} W_j(\varphi)$, which is the average distribution function of the chain. Let us take the limit $N \to \infty$ and denote $\mathbf{W}(\varphi) = \lim_{N\to\infty} W^N(\varphi)$. It is not hard to see that this function will satisfy:

$$\mathbf{W}(\varphi) = \sum_{i=1}^{m} p_i \left\{\mathbf{W}\left(\mathcal{T}_i^{-1}(\varphi)\right) - \mathbf{W}\left(\mathcal{T}_i^{-1}(0)\right)\right\} \quad \text{(B.18a)}$$
$$\mathbf{W}(\varphi + r\pi) = \mathbf{W}(\varphi) + r \quad \text{(B.18b)}$$
$$\mathbf{W}(\pi) = 1 \quad \text{(B.18c)}$$
$$\mathbf{W}(\varphi) \text{ is an increasing function of } \varphi \quad \text{(B.18d)}$$

with $\varphi \in (0, \pi]$. And,

$$\langle \Delta\varphi \rangle = \sum_{i=1}^{m} p_i \int_0^{\pi} \frac{\mathrm{d}\mathbf{W}(\varphi)}{\mathrm{d}\varphi} \left\{\mathcal{T}_i(\varphi) - \varphi\right\} \mathrm{d}\varphi. \quad \text{(B.19)}$$

Schmidt has proved [11] that the solution of equations (B.18) for each energy is unique and continuous. To carry out the integration in (B.19) we use the existence of a value $\varphi_0 = \frac{\pi}{2}$ such that $\mathcal{T}_i(\varphi_0)$ verifies $\mathcal{T}_i(\varphi_0) \equiv \varphi_1 = \pi$ for any species a_i.

$$\langle \Delta\varphi \rangle = \sum_{i=1}^{m} p_i \int_0^{\pi} \frac{\mathrm{d}\mathbf{W}(\varphi)}{\mathrm{d}\varphi} \left\{\mathcal{T}_i(\varphi) - \varphi\right\} \mathrm{d}\varphi$$
$$= \sum_{i=1}^{m} p_i \int_{\varphi_0}^{\varphi_0+\pi} \frac{\mathrm{d}\mathbf{W}(\varphi)}{\mathrm{d}\varphi} \left\{\mathcal{T}_i(\varphi) - \varphi\right\} \mathrm{d}\varphi\,,$$

integrating by parts

$$\langle \Delta\varphi \rangle = \sum_{i=1}^{m} p_i \mathbf{W}(\varphi) \left\{\mathcal{T}_i(\varphi) - \varphi\right\} \Big|_{\varphi_0}^{\varphi_0+\pi}$$
$$- \sum_{i=1}^{m} p_i \int_{\varphi_0}^{\varphi_0+\pi} \mathbf{W}(\varphi) \frac{\mathrm{d}\mathcal{T}_i(\varphi)}{\mathrm{d}\varphi} \mathrm{d}\varphi + \sum_{i=1}^{m} p_i \int_{\varphi_0}^{\varphi_0+\pi} \mathbf{W}(\varphi) \mathrm{d}\varphi,$$

and using (B.18a)

$$\sum_{i=1}^{m} p_i \int_{\varphi_0}^{\varphi_0+\pi} \mathbf{W}(\varphi) \frac{\mathrm{d}\mathcal{T}_i(\varphi)}{\mathrm{d}\varphi} \mathrm{d}\varphi$$
$$= \sum_{i=1}^{m} p_i \int_{\varphi_1}^{\varphi_1+\pi} \mathbf{W}\left(\mathcal{T}_i^{-1}(\theta)\right) \mathrm{d}\theta$$
$$= \int_{\varphi_1}^{\varphi_1+\pi} \mathbf{W}(\theta) \mathrm{d}\theta + \pi \sum_{i=1}^{m} p_i \mathbf{W}\left(\mathcal{T}_i^{-1}(0)\right).$$

Going back to the expression for $\langle \Delta\varphi \rangle$ we obtain:

$$\langle \Delta\varphi \rangle = (\varphi_1 - \varphi_0) - \pi \sum_{i=1}^{m} p_i \mathbf{W}\left(\mathcal{T}_i^{-1}(0)\right)$$
$$+ \int_{\varphi_0}^{\varphi_0+\pi} \mathbf{W}(\varphi) \mathrm{d}\varphi - \int_{\varphi_1}^{\varphi_1+\pi} \mathbf{W}(\theta) \mathrm{d}\theta.$$

From (B.18b) it is easy to see that

$$\int_{\varphi_0}^{\varphi_0+\pi} \mathbf{W}(\varphi) \mathrm{d}\varphi - \int_{\varphi_1}^{\varphi_1+\pi} \mathbf{W}(\theta) \mathrm{d}\theta = \varphi_0 - \varphi_1$$

and finally the following relationship holds for a certain value ϵ of the energy:

$$\frac{\langle \Delta\varphi \rangle}{\pi} \equiv \mathcal{K} = -\sum_{i=1}^{m} p_i \mathbf{W}\left(\mathcal{T}_i^{-1}(0)\right). \quad \text{(B.20)}$$

Solving the equations (B.18) for different values of ϵ one can calculate the density of states of the random chain from

$$G(\epsilon) = \frac{\left|\mathcal{K}\left(\epsilon + \frac{\Delta\epsilon}{2}\right) - \mathcal{K}\left(\epsilon - \frac{\Delta\epsilon}{2}\right)\right|}{\Delta\epsilon}. \quad \text{(B.21)}$$

References

1. R. de L. Kronig, W.G. Penney, Proc. Roy. Soc. A **130**, 499 (1931)
2. E.H. Lieb, D.C. Mattis, *Mathematical Physics in one dimension* (Academic Press, 1966). We strongly suggest this book to the interested reader. It contains a large amount of seminal reprinted articles as well as huge number of crucial references
3. S.L. Altmann, *Band theory of solids: an introduction from the point of view of symmetry* (Oxford University Press, 1991)
4. F. Szmulowicz, Eur. J. Phys. **18**, 392 (1997)
5. C. Dekker, Phys. Today **52**, 22 (1999)
6. D. Saxon, R. Hutner, Philips Res. Rep. **4**, 81 (1949)
7. H. Hegger, B. Huckestein, *et al.*, Phys. Rev. Lett. **77**, 3885 (1996)
8. S. Flugge, *Practical Quantum Mechanics* (Springer Verlag, 1971), Vol. 1, pp. 64–68
9. R.L. Agacy, R.E. Borland, Proc. Phys. Soc. **84**, 1017 (1964)
10. J.M. Luttinger, Philips Res. Rep. **6**, 303 (1951)
11. H. Schmidt, Phys. Rev. **105**, 425 (1957)
12. H. James, A. Ginzbarg, J. Phys. Chem. **57**, 840 (1953)
13. J.E. Gubernatis, P.L. Taylor, J. Phys. C **4**, L94 (1971)
14. P.W. Anderson, Phys. Rev. **109**, 1492 (1958)
15. D.H. Dunlap, H-L. Wu, P.W. Phillips, Phys. Rev. Lett. **65**, 88 (1990)
16. A. Sánchez, E. Maciá, F. Domínguez-Adame, Phys. Rev. B **49**, 147 (1994)
17. V. Bellani, E. Diez, R. Hey, L. Tony, L. Tarricone, G.B. Parravicini, F. Domínguez-Adame, R. Gómez-Alcalá, Phys. Rev. Lett. **82**, 2159 (1999)
18. R.E. Borland, Proc. Roy. Soc. A **274**, 529 (1963)
19. M.Ya. Azbel, P. Soven, Phys. Rev. Lett. **49**, 751 (1982)